Histochem Cell Biol (1997) 108:67–75

ORIGINAL PAPER

Jekaterina Erenpreisa · Talivaldis Freivalds
Helmtrud Roach · Roger Alston

Apoptotic cell nuclei favour aggregation and fluorescence quenching of DNA dyes

Accepted: 12 February 1997

Abstract Apoptotic cell nuclei are known to stain hyperchromatically with absorption dyes and dimly with many DNA fluorochromes. We hypothesised that both optical phenomena have the same cause - the ability of apoptotic chromatin to aggregate cationic dyes. This hypothesis was tested using prednisolone-primed rat thymus, which is known to contain apoptotic cells. The apoptotic cells were classified as early and late, based on their morphology, in thin and semithin sections and in thymus imprints on slides. Direct reaction for DNA strand breaks (TUNEL) indicated the presence of breaks in both categories of cells, with more intense labelling in late apoptosis. The chromatin ultrastructure of early apoptotic cells initially retained the supranucleosomal order of packaging which characterises control cells, whereas the dense chromatin of late apoptotic cells possessed the degraded structure. Absorption spectra of the toluidine blue-stained early apoptotic cell chromatin revealed a metachromatic shift, indicating a change of DNA conformation and polymerisation of the dye. When the staining was performed by acridine orange (preceded by a short acid treatment), a paradoxical several-fold increase of fluorescence intensity at a several-fold dilution of the dye was found. The simultaneous reduction of the ratio of red to green components of fluorescence confirmed that the concentration-dependent fluorescence quenching was due to aggregation of the dye. The results suggest that the enhanced affinity of the chromatin of early apoptotic cells for cationic dyes is associated with conformational relaxation rather than degradation of DNA. In late apoptotic cells, the very dense packaging of degraded DNA promotes further aggregation of dyes. The results suggest alternative methods for detection and discrimination of early and late apoptotic cells.

J. Erenpreisa (✉)
A. Kirchenstein Institute, Ratsupites strasse1, Riga LV-1067, Latvia
Tel. +3712 426361; fax +3712 428036
e-mail cancer@laima.acad.latnet.lv

T. Freivalds
Institute of Experimental and Clinical Medicine, Riga LV-1004, Latvia

H. Roach · R. Alston
Southampton University, SO 16 6YD, UK

Introduction

There is much interest in methods for detecting apoptosis, the main mode of programmed cell death. The cleavage of DNA by endonucleases is known to represent the biochemical hallmark of apoptosis and can be demonstrated in DNA gel electrophoresis as a “ladder” (Wyllie et al. 1981). The DNA strand-breaks can be directly detected in situ using DNA polymerase- or terminal transferase-primed chain reactions with especially elaborated kits. These, although sensitive, are, however, time-consuming and costly reactions. Among indirect methods, the presence of a sub-G_0+G_1 peak in DNA histograms, detected by DNA fluorochromes, is the most widely accepted cytometric feature to establish the presence of an apoptotic fraction among fixed or detergent-treated cells (Telford et al. 1992; Pellicciari et al. 1993). The mechanism of this reduced fluorescence employing a variety of fluorochromes with different mechanisms of binding to DNA remains unclear (Telford et al. 1992). Loss of endonuclease-fragmented DNA is certainly one of the reasons (Darzynkiewicz et al. 1992; Hotz et al. 1994). However, data are now available that show that oligomeric DNA fragmentation is a late event, coinciding with the disintegration of apoptotic cells, while the preceding chromatin condensation correlates with the large-scale, 300–50 kb, fragmentation of DNA (Ghibelli et al. 1995; McConkey et al. 1996). The latter can hardly cause any substantial loss of DNA. Therefore, some authors supposed that early changes of chromatin texture and stainability may be responsible for the changed fluorescence of apoptotic cells (Lieger et al. 1995; Ferlini et al. 1996).

Apoptotic chromatin is very dense. Telford et al. (1992) speculated that it might, therefore, exclude the dyes. However, this contradicts the hyperchromatic staining of apoptotic nuclei with absorption cationic dyes of various

chemical structures and DNA staining mechanisms, e.g. haematoxylin, azure, silver methenamine. Hyperchromasia of dense small nuclei, known as karyopycnosis, has been, and still is, used by pathologists to count degenerated cells. Thus, apoptotic cell nuclei do not exclude, but, on the contrary, seem avidly to bind the dyes, which is why we suggested that the low emission of apoptotic chromatin when stained with fluorescent dyes was due to oversaturation with dye molecules. The high density of the dye per substrate may cause fluorescence quenching (Förster and König 1957). This was clearly demonstrated on biological specimens, applying a variety of widely used fluorochromes (Entwistle and Noble 1992).

With absorption dyes, the same aggregation would cause an increase of optical density (hyperchromasia) of the stained substrate. Thus, in both the cases, the stoichiometry of DNA staining becomes altered. Aggregation of the dye molecules (if planar and mono-charged), is accompanied by their polymerisation on the regularly arranged chromatin, manifesting the so-called metachromasia (change of colour) (Michaelis 1947; Sculthore 1978) and birefringence (Fisher and Romhanyi 1977; Erenpreisa 1989).

The present study was carried out to investigate whether the physico-chemical properties of apoptotic chromatin favour the aggregation of the dyes. Does apoptosis cause metachromasia, birefringence and the concentration-dependent loss (quenching) of fluorescence, and are these effects associated with the cleavage of DNA? These questions were addressed and answered in the affirmative.

Materials and methods

Animals and tissue preparation

The in vivo model of prednisolone-primed rat thymus apoptosis was used (Ansari et al 1993). The experiments on animals were conducted in accordance with the fundamental principles of the international ethical code promulgated by CIOMS (Recueil de Legislation Sanitaire, 36/2, 1985, Geneva). In 13 experiments, prednisolone succinate (or saline) was injected into 3 to 4-week-old Wistar rats i.p. 5 mg/kg. After 2–4 h, the treated animals were killed with ether. Immediately, cell imprints of the dissected thymus glands were made by pressing the tissue gently onto slides. These were dried for 5 min and either fixed in ethanol:acetone (1:1) at 4°C for 30 min or, for the direct detection of DNA strand breaks, in methanol:acetone at –20°C for 10 min. The latter were dried and preserved until use in a desiccator at 4°C.

Staining

Two cationic DNA binding dyes were used, the fluorochrome, acridine orange (AO, Sigma) and the absorbing thiazine dye, toluidine blue (TB, Gurr). Both are capable of metachromasia. Staining with TB was performed as follows: the cell imprints with ethanol/acetone fixation were dried and stained (with and without preceding RNase and short acid treatments) in 0.05% TB solution in 50% citrate-phosphate (McIlvain) buffer pH 4.0 at room temperature for 10 min, briefly rinsed in distilled water, blotted with filter paper, passed through warm tertiary butanol and Histoclear (3 min×2 in each) and mounted in DPX.

AO staining was preceded by a short treatment with HCl (HCl-AO). In this test, the apoptotic DNA acquires a metachromatic red colour while non-apoptotic cell nuclei retain an orthochromatic green fluorescence. The test is usually applied in flow cytometric analysis (Darzynkiewicz 1994). Here the method was adjusted for visual observation (requiring a higher concentration of AO) following the early recommendations of Rigler (1966) and Roschlau (1965) with the following modifications. After the 30-min cold fixation in ethanol/acetone (in some experiments, fixation was prolonged at 4°C overnight), the slides were passed through decreasing grades of ethanol to PBS. The slides were then treated with 20 mg/ml, pre-boiled RNase A (Sigma) in PBS (37°C, 30 min), rinsed in PBS, hydrolysed in 1 N HCl (60°C, 30 s), washed in three changes of distilled water (1 min each), passed through PBS and 0.1 M acetic buffer pH 4.1 (5 min), stained with 10^{-4} M AO in the same buffer for 15 min, passed through three changes (5 min each) of AO diluted to 10^{-6} M in the same buffer and sealed in the latter solution under a glass cover slip with nail polish (moviol and glycerol cannot be used).

For investigations of the staining mechanisms, some variations were used: RNase was omitted; HCl treatment was omitted or used at greater dilution and for briefer times (e.g. 0.1 N HCl, room temperature, 30 s). HCl treatment was also substituted with 0.4 M NaCl, 0.1% Triton X-100, 4°C, 5 min to facilitate extraction of labile basic chromatin proteins (Erenpreisa 1990). The AO concentration was varied from 2×10^{-4} M to 0.05×10^{-4} M.

As positive and negative controls, sensitising and removing treatments with DNase (sDNase and rDNase, respectively) were used with an additional check by the Feulgen reaction. For the positive control, 10 U/ml RNase-free DNase I (in 30 mM TRIS-HCl pH 7.2, 140 mM sodium cacodylate, 1% BSA, 4 mM $MgCl_2$, 0.025 mM $CoCl_2$, 0.1 mM dithiothreitol) was applied for 1 h at room temperature. For the complete removal of the DNA, crude DNase I (Sigma), 200 U/ml (in PBS containing 45 mM $MgCl_2$, 0.1 mM dithiothreitol) was applied at 37°C for 1 h.

TUNEL reaction detecting DNA strand breaks

This was carried out according to the method of Gavrieli et al. (1992) with some modifications. The cell imprints on slides were incubated under cover-glasses for 1 h at 37°C with 25 µl of the end-labelling buffer (30 mM TRIS-HCl pH 7.2, 1% BSA, 140 mM sodium cacodylate, 1 mM $CoCl_2$) containing 1 µl dNTPs (digoxigenin-DNA labelling mix with labelled dUTP, Boehringer Manheim) and 5 or 7.5 U of terminal deoxynucleotidyl transferase (tdT). The reaction was stopped with 0.1 M TRIS-HCl buffer containing 30 mM NaCl and 30 mM sodium citrate. After extensive washing, the incorporation of digoxigenin-labelled dUTP was detected using monoclonal anti-digoxigenin Fab fragments linked directly to alkaline phosphatase (ALP; Boehringer Mannheim, 1:1000 dilution, 1–2 h incubation), followed by colour development with nitro blue tetrazolium/BCIP for 40 min. Alternatively, a secondary antibody was linked to peroxidase, which was visualised using 3-amino-9-ethylcarbazole as a substrate.

Microspectrophotometry

Microspectrophotometry was carried out on stained cell imprints with an MPV-3 (Leica). TB spectra were taken using a plug area of 1 μm^2, a monochromator split of 0.15 µm and a step of 4 nm. For each spectral point, 128 measurement repetitions were made automatically and the average recorded. For each cell type, 7–12 spectra were collected, averaged and normalised. To study AO fluorescence, the emission intensity of the whole nucleus was measured adjusting a plug to the nuclear size, in 12 cells of each group, at 540 nm for green and at 640 nm for red fluorescence (monochromator split 1 µm). For these experiments, which were repeated 3 times, the main scheme of HCl-AO staining was applied. Confocal microscopy was carried out with a TCS 4D (Leica), using a krypton/argon laser. The exitation wavelength was

488 nm. Applying a narrow band-pass and a 590-nm long-pass barrier filter, two distinct wavelength emissions were obtained, one between 515 and 545 nm (in the green area of the spectrum) and the other above 590 nm (in the red area of spectrum). A series of eight dual-channel optical sections was taken, the four intermediate ones were then combined into a 3D image. The final confocal images had the considerable advantage of an almost complete elimination of flare and an increase in resolution.

Electron Microscopy

Small pieces of thymus were fixed with 3% glutaraldehyde in 0.1 M cacodylate buffer (pH 7.2) containing 2 mM $CaCl_2$. Postfixation was carried out in 1% buffered osmium tetroxide and aqueous uranyl acetate, followed by embedding in Spurr resin. Thin sections were contrasted with lead citrate.

Results

Electron microscopy

The thymus of juvenile rats contained about 7–15% of apoptotic cells, as had also been found by Ansari et al. (1993). Apoptotic cells were much more numerous in the thymus of prednisolone-treated rats (Fig. 1), where the whole gamut of transition steps to apoptosis was observed. Two main stages could be distinguished:

1. The nuclei lacked diffuse chromatin, while the compact chromatin with a supranucleosomal structure extended evenly throughout the nuclear interior (Figs. 1, 2a). They retained the supranucleosomal organisation of the chromatin up to the late stage of apoptosis. These cells were classified as “early apoptotic cells”.
2. “Late apoptotic cells” were very small, possessing dense “non-transparent” chromatin, which sometimes segregated into crescents and caps (Fig. 1). They disintegrated into apoptotic bodies and were engulfed by numerous macrophages. At high power transmission electron microscopy (TEM), their chromatin displayed a very dense altered texture (Fig. 2b).

Fig. 1 Semithin section (**a**) and low power transmission electromicrograph (TEM); **b** of prednisolone-treated rat thymus. (*Asterisk* T-lymphoblast, *stars* early apoptotic cells, *arrows* late apoptotic cells) Magnification for **a**×2000, *bars* 4.5 μm

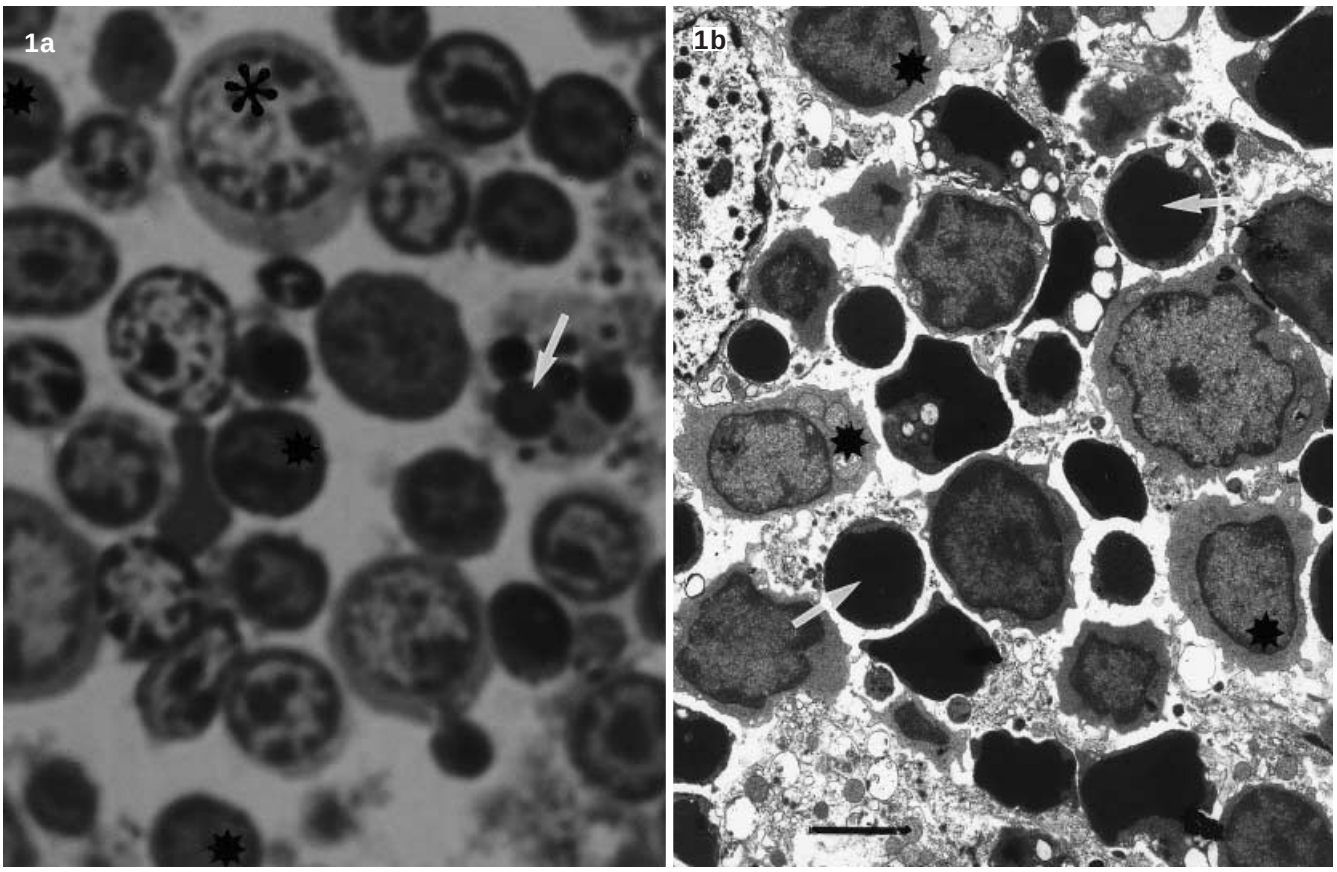

TUNEL reaction

The number of cells with positively labelled nuclei was, on the whole, similar to the number of hyperchromatic and karyopycnotic cells counted in TB-stained semithin sections, thus pointing to the relevance of both counts (Figs. 3, 4). However, TUNEL labelling detected by the ALP reaction depended on the thickness of the cell smear and on the concentration of TdT. In thick smears with an enzyme concentration of 7.5 U/slide, it had a tendency to stain both early and late apoptotic cells with similar intensities. In thin smears or at an enzyme con-

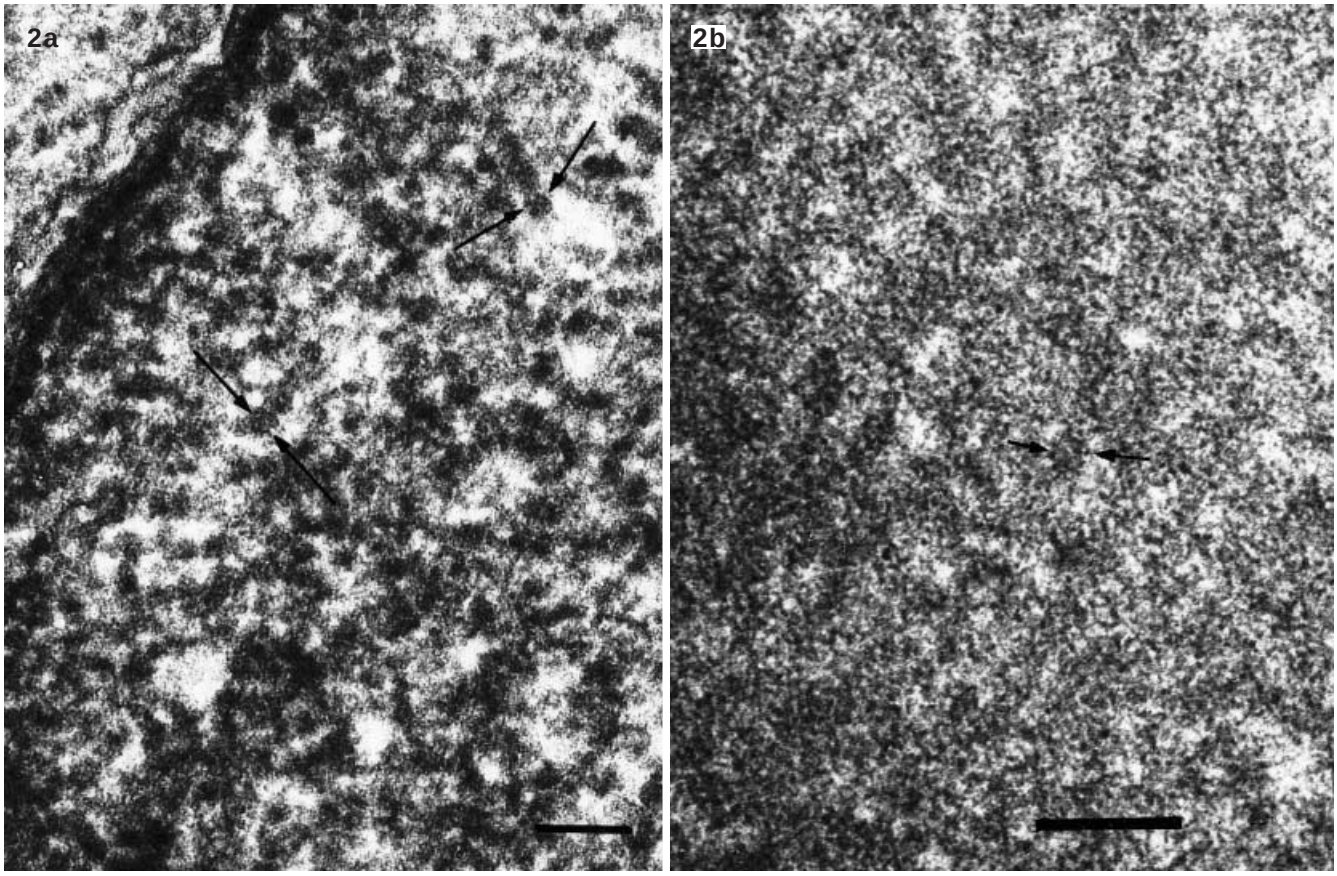

Fig. 2a, b High power TEM showing the texture of apoptotic chromatin. **a** The nucleus of an early apoptotic cell. The coiled chromatin threads of the supranucleosomal level of organisation, textured as 30-nm globules, are seen (*arrows*). *Bar* 100 nm. **b** The nucleus of a late apoptotic cell. The chromatin is degraded and very dense. Contours of deteriorating (fuzzy) nucleosomes can only be assessed (*arrows*). *Bar* 50 nm.

centration of 5 U, only late apoptotic cells reacted (Fig. 3). The TUNEL reaction, visualised by the peroxidase method with a TdT concentration of 5–7.5 U/slide, was less dependent on the thickness of the cell imprint. Late apoptotic cells were labelled heavily while early apoptotic cells were only weakly labelled. sDNase treatment resulted invariably in a positive reaction in all cells at enzyme concentrations of 5–7.5 U/slide, whereas rDNase abolished any label.

TB staining

The number of karyopycnotic cells on cell imprints approximately coincided with that detected in parallel semithin sections. In both cell imprints and semithin sections of a prednisolone-treated thymus, stained with TB pH 4, the main categories of thymocytes, blasts, early and late apoptotic cells, could be clearly discerned (Fig. 1a). The nuclei of apoptotic cells showed, on cell imprints, hyperchromasia and some birefringence. Both increased after sDNAse or short acid treatment. Applying both treatments, strong hyperchromasia and birefringence were achieved (Figs. 5, 6). RNase had very little impact on the amount of nuclear staining of T-lymphocytes. rDNase fully removed nuclear staining with TB.

Spectrophotometry of T-lymphocyte chromatin (Fig. 7) showed that: (1) in control T-lymphocytes, the spectrum maximum was constant (570 nm) and independent of the density of the measured chromatin patch data (not presented), indirectly indicating the stoichiometry of the staining method; (2) early apoptotic cells displayed a hypsochromic metachromatic shift of spectrum maximum by 20 nm; and (3) in late apoptotic cells, there was a further hypsochromic shift to even shorter wavelengths. In addition, an exaggerated batochromic shoulder appeared at 640 nm. As a result, a very broad spectrum of absorption was formed.

Fig. 3 Direct reaction for DNA strand-breaks (TUNEL visualized by the alkaline phosphatase method) on prednisolone-treated thymus cell imprint. ×700 ▶

Fig. 4 Semithin section of the same thymus as in Fig. 3. Toluidine blue (TB) staining. The number of late apoptotic (karyopycnotic) cells (25–30%) is comparable to the number of TUNEL-labelled cells. ×700

Fig. 5 Hyperchromatic staining of thymus cell nuclei with TB (pH 4) after sensitising DNase and short acid treatments, mimicking apoptotic cells. Cell imprint. ×1120

Fig. 6 Birefringence of a similar sample as in Fig. 5 when viewed under crossed polarisers. ×1120

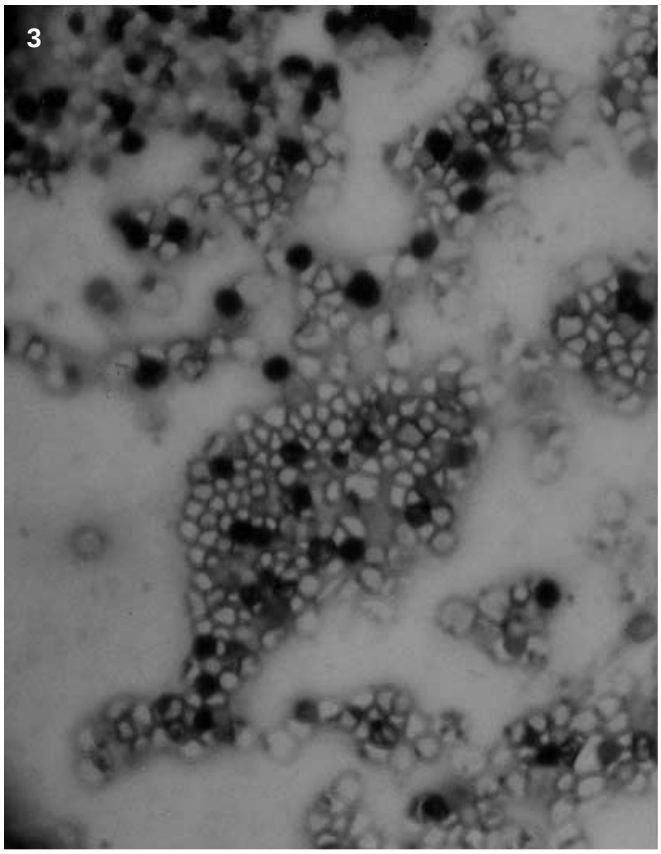
3

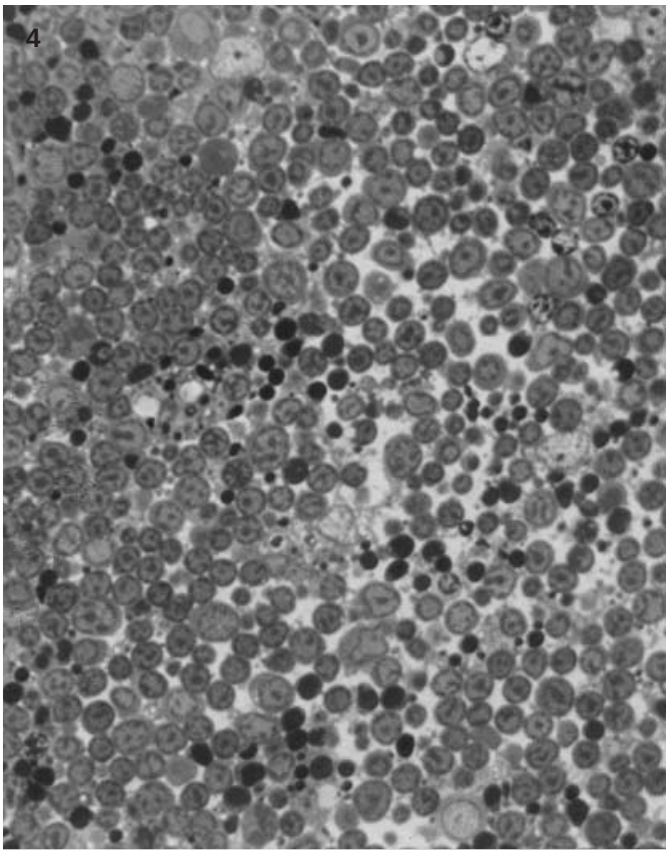
4

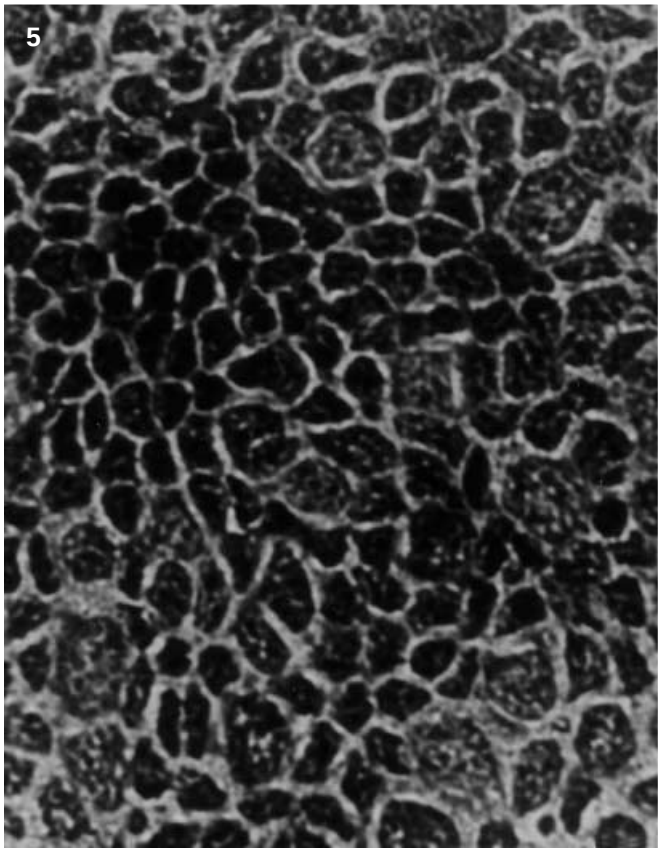
5

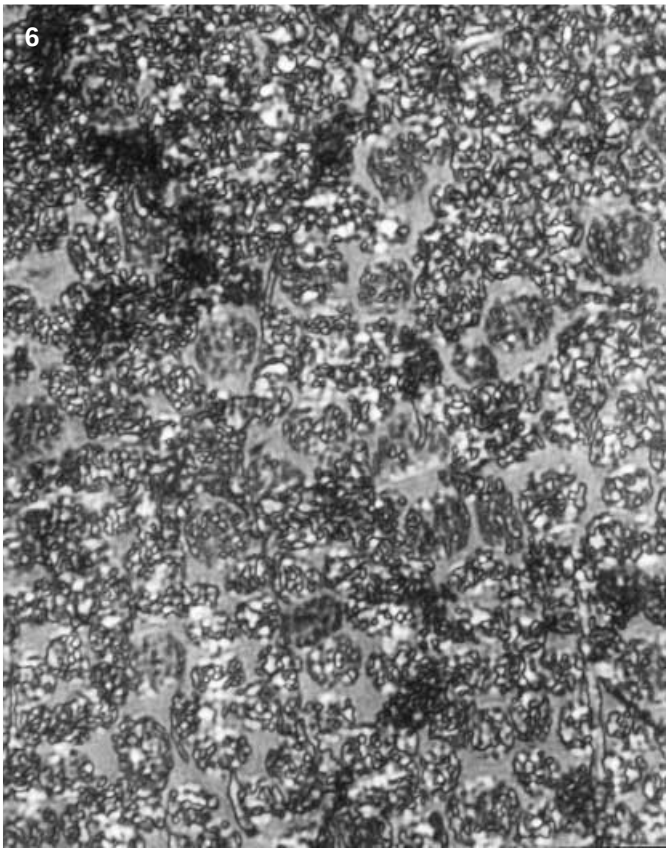
6

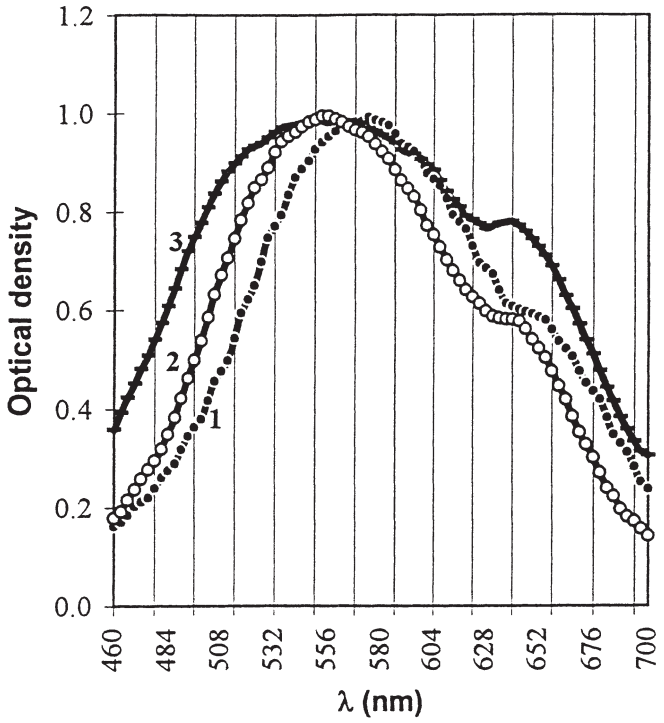

Fig. 7 Normalised averaged spectra of TB (pH 4)-stained nuclear chromatin in: (*1*) control rat T-lymphocytes, (*2*) early and (*3*) late apoptotic cells of the prednisolone-treated rat thymus. The morphology of relevant early and late apoptotic cells is shown in Fig. 1a

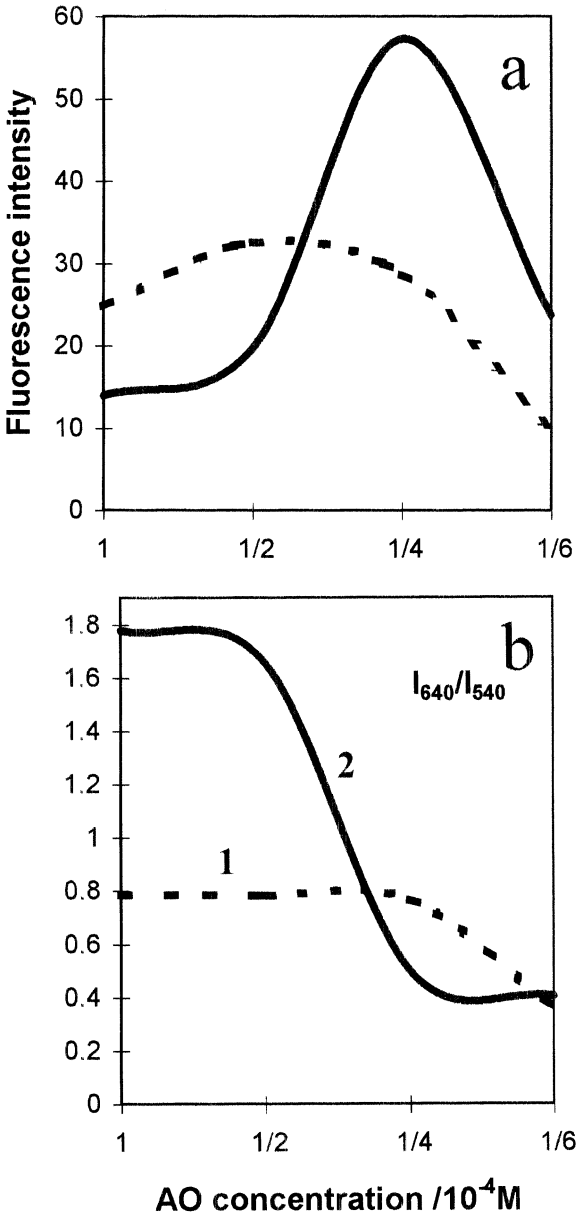

Fig. 8a, b Dependence of the nuclear fluorescence on acridine orange (*AO*) concentration in cells of prednisolone-treated rat thymus when stained by the HCl-AO method. **a** Early apoptotic cells: the intensity of green emission is shown by a *continuous line* and of the red emission by *discontinuous line*. **b** Ratio of red to green fluorescence intensities. *1* T-lymphoblasts, *2* early apoptotic cells. The morphology of the relevant cells, numbered *1* and *2* correspondingly, is shown in Fig. 10

HCl-AO method

In control rats, the predominant colour of thymus imprints was light orange-yellow-greenish but here and there “red eyes” of apoptotic cell nuclei sparkled (Fig. 9a). About 60% of quiescent T-lymphocyte nuclei possessed some red component in the spectrum of staining, assigning them yellow or light orange fluorescence. After removal of nuclear RNA with RNase, which could be substituted by more prolonged acid treatment (1 N HCl, 60°C, 1 min), the large nuclei of cycling T-lymphoblasts had very little red component in their fluorescence and stained prevalently green (Fig. 9). RNase treatment did not alter substantially the pattern of staining of T-lymphocytes.

In prednisolone-treated animals, the predominant tissue fluorescence shifted to purple-orange, while the green blasts stood out. The majority of T-lymphocytes possessed dim orange or red-spotted nuclei (Fig. 10). Their density in phase contrast was greater than in control cells. Their number parallelled those defined as early apoptotic cells in TB-stained semithin sections, cell imprints and by TUNEL reactions. The number varied, depending on the animal and time of glucocorticoid exposure, from 40 to 60%.

In the process of apoptosis, the green intercalation fluorescence of cell nuclei diminished proportionally to the increase of the red external staining. Late apoptotic cell nuclei with clear red chromatin lumps lacked the green component in their emission spectrum (Fig. 9). Their number in prednisolone-treated animals comprised 25–40%. When apoptosis was very rapid, dark patches were seen in the red-spotted nuclei of most T-lymphocytes but some nuclei of late apoptotic cells became dim red or contained “black holes” (Fig. 10). These were of low density in phase contrast, indicating loss of the substrate. To a lesser extent, the appearance of black holes

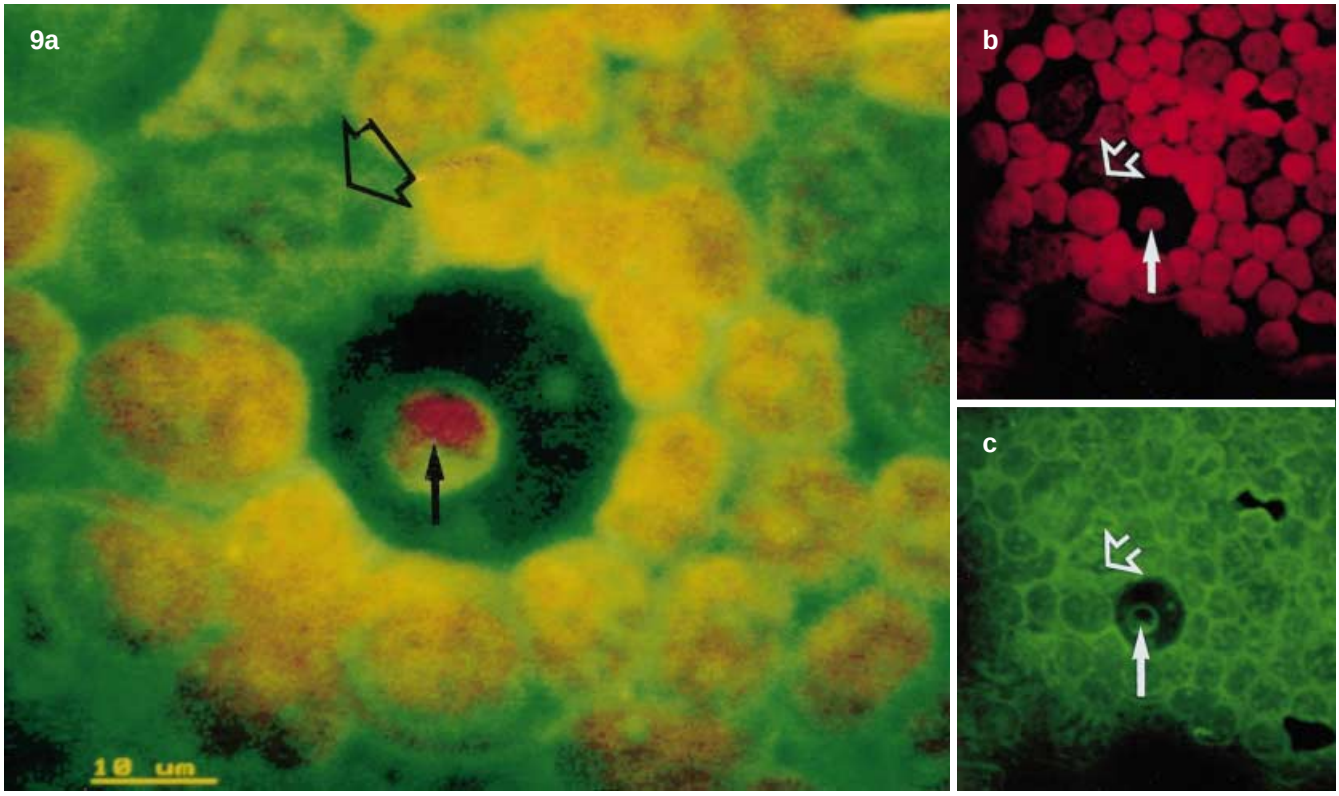

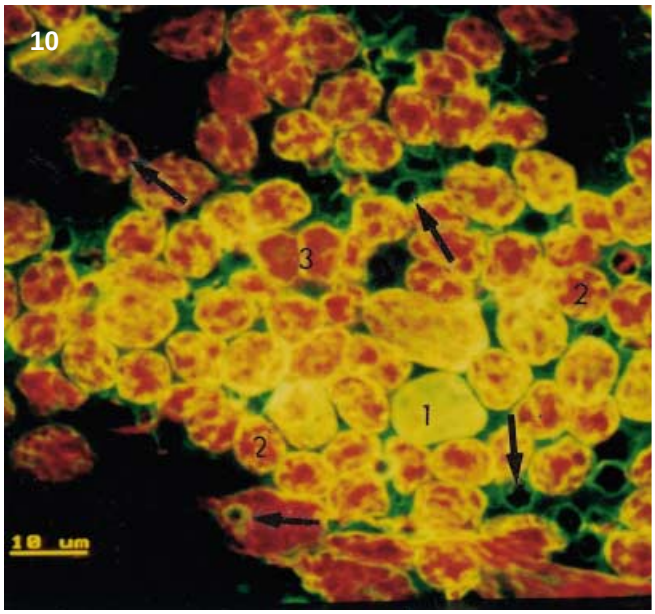

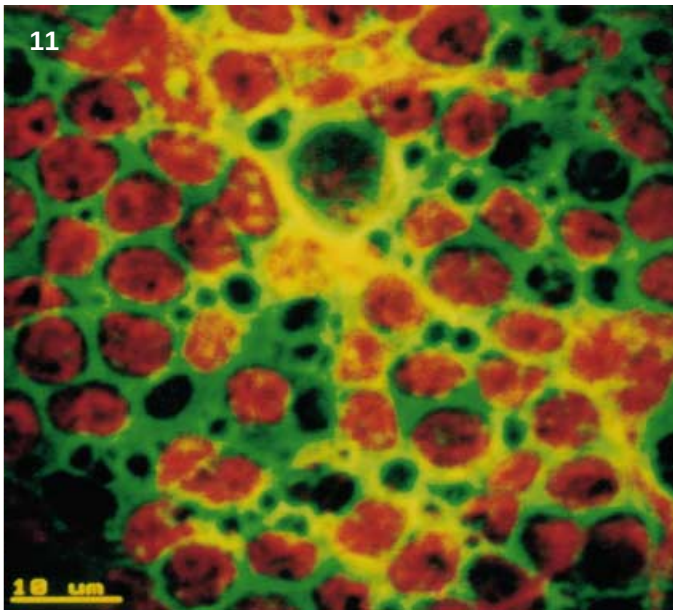

Fig. 9a–c A cell imprint of the control thymus stained with HCl-AO. Reconstruction of the dual-channel confocal sections. Light orange nuclei belong to quiescent T-lymphocytes. An apoptotic cell with a red clump of highly degraded chromatin is indicated by the *thick arrow*. A T-lymphoblast nucleus possessing green fluorescence is shown by the *broad arrow*. This same image is separated in the red and green channels (**b**, **c**). The red lump of degraded chromatin lacks the green component, quiescent T-lymphocytes possess green and red fluorescence in an approximately 50:50 ratio, while the T-lymphoblast nucleus has only a very low red component

Fig. 10 Cell imprint of prednisolone-treated thymus stained with the HCl-AO method. Except for one non-apoptotic T-lymphoblast which stains green-yellow (*1*), all T-lymphocytes are in the process of apoptosis and show either red spots (*2*) during the early stages of apoptosis or stain entirely red (*3*) in the late stages of apoptosis. Note also some "black holes" which might indicate loss of substrate plus fluorescence quenching (*arrows*)

Fig. 11 Sensitsing sDNase applied to a cell imprint of rat thymus before staining with HCl-AO. The nuclei are bright red due to introduced DNA strand breaks, thus displaying a positive control for apoptosis

depended on the duration of fixation or the intensity of acid hydrolysis.

The green fluorescence of T-lymphoblasts remained unchanged in prednisolone-treated animals. After sDNase treatment, applied as a positive control to induce DNA breaks, all nuclei stained red (Fig. 11).

Using modifications of the main staining scheme, it was established that:

1. Any short acid treatment provided visually differential staining of apoptotic, quiescent and blastic cells. The acid treatment could be substituted with 0.4 M NaCl.
2. The visually differential staining for apoptotic cells could be obtained at the pH used only within a limited range of AO concentrations, from 2×10^{-4} to 0.5×10^{-4} M. With more diluted dye solutions, all cell nuclei became brilliant greenish-yellow and many holes vanished. Spectrofluorometry of the early apoptotic cell nuclei showed (Fig. 8a) that at a fourfold dilution the intensity of AO green fluorescence increased fivefold, the red component also increased but less significantly (by 35% at threefold dilution). Correspondingly, the ratio of the red to the green component dropped dramatically (Fig. 8b).
3. The spectrum of T-lymphoblast nuclei, measured in the same imprints, was effectively unchanged over the AO dilution range examined (Fig. 8b).

Discussion

The induction of apoptosis in T-lymphocytes by prednisolone was confirmed by ultrastructural morphology and the accumulation of DNA strand breaks, as demonstrated by the TUNEL reaction. Both the chromatin structural probes, with HCl-AO and TB, showed a metachromatic change in the staining spectrum of apoptotic chromatin. This shift was already apparent in early apoptotic cells. Together with the polarisation of staining this indicated a conformational change of DNA and an aggregation of dye molecules on the regularly arranged chromatin (Michaelis 1947; Fisher and Romhanyi 1977). Both the dye aggregation and TB birefringence of apoptotic cell nuclei could be induced by sDNase treatment, which mimicked the main event of apoptosis, cleavage of DNA. In addition, the batochromic peak of TB spectrum in late apoptotic cells indicated further disordered aggregation of the dye (Erenpreisa et al. 1992).

The results of cytospectrofluorometry when staining with decreasing concentrations of AO showed a paradox: a very high increase of fluorescence intensity at a several-fold dilution of the dye. The ratio of intensities of the red metachromatic fluorescence to the green reduced drastically. There may be two explanations: either the staining mechanism shifted from external cooperative binding of DNA phosphate groups (red) for intercalation (green) or the orthochromatic fluorescence was released from quenching by diminishing aggregation of the dye (any binding of AO to nucleic acids may produce green orthochromatic fluorescence if the dye is not polymerised).

The first alternative is contradicted by some increase of red fluorescence preceding the green flare and a several-fold increase of the sum of red and green fluorescence in diluted AO. The latter indicates severe non-linearity of staining (oversaturation with the dye) and quenching of fluorescence on apoptotic chromatin in the concentrated dye solution. Absence of this phenomenon in T-lymphoblasts, which had not undergone DNA cleavage, confirmed that the dye aggregation and fluorescence quenching were associated with the intrinsic properties of apoptotic chromatin.

The findings suggest the possibility of some new methodical approaches:

1. The proportion of early and late apoptotic cells might be estimated by cytometry, applying monochromatic cationic DNA fluorophores at saturating and undersaturating concentrations (the early apoptotic cells will join late ones in a sub-G_0+G_1 peak only at saturation and will shift to G_0+G_1or a hyperdiploid peak at undersaturation).
2. The drop in the red to green fluorescence ratio, which occurs when diluting the dye from saturating to undersaturating concentrations in the HCl-AO method, may represent a measure of DNA cleavage (the ability to aggregate the dye). This method would not need any calibration of fluorescence intensities in the red and green channels in relation to an independent cell control.

While quenching of fluorescence by the aggregated dye potentiates the decrease of fluorescence due to the loss of DNA in late apoptotic cells, aggregation of the absorption dye, caused by the same cleavage of DNA, compensates for it. This endorses the value of the "old-fashioned" karyopycnotic index, applying simple nuclear stains for detecting late apoptotic cells.

There arises the question as to why apoptotic chromatin binds cationic dyes so avidly? As we found, this ability appeared in early apoptotic cells. Both early and late apoptotic cells contain DNA breaks, though in different numbers. The texture of the chromatin of early apoptotic cells, as seen in TEM, indicated that the regular supranucleosomal order of DNA packaging was initially retained. Therefore, one could envisage that the differential staining of early apoptotic cells arose from an impairment of the higher, loop-domain level of DNA folding.

It is established that these large (50 kb) segments of the genome represent the units of conformational transitions of DNA: even one single-strand break causes relaxation of the supertwisted closed DNA loop domain (Stryer 1988). This suggests that a very limited number of strand breaks can convert a supertwisted conformation of DNA into the relaxed one. Therefore, the cytochemical properties of the chromatin of early apoptotic cells are likely to be associated with conformational relaxation rather than degradation of DNA. This is supported by the pattern of DNA fragmentation into precisely 50-kb segments, being the predominant size of fragments up to late apoptosis (McConkey et al. 1996). The enhanced stainability of the chromatin with cationic dyes and electron microscopy contrastants, found earlier by introducing single-strand breaks into DNA of live tumour cells

(Erenpreisa et al. 1988), is also in agreement with this suggestion. The easier exposure of DNA phosphates, provoked either by short acid or 0.4 M NaCl treatment, may be explained by weaker DNA-protein interactions in the relaxed chromatin.

In conclusion, the ability of apoptotic chromatin to cause aggregation was shown here for two cationic dyes, one absorption and another fluorescent, each staining DNA by different mechanisms: TB, external only, AO, both intercalating and external. This suggests that the phenomenon of dye aggregation by the chromatin represents a general feature of apoptotic cells. It is caused by DNA cleavage and therefore can be used in indirect methods for detection of DNA strand breaks and apoptosis.

Acknowledgements The authors gratefully acknowledge the support of the Royal Society for the collaboration between Southampton and Riga. We also greatly appreciate the technical assistance of Miss. Sue Cox and Mr. Nick Barnett at the EM Unit, and Mr. Adrian Wilkins at the Academic Unit in Southampton, as well as Mr. Vladislavs Zelchs of the EM Unit in Riga.

References

Ansari B, Coates PJ, Greenstein BD, Hall PA (1993) In situ end labelling detects DNA strand breaks in apoptosis and other physiological and pathological states. J Pathol 170:1–8

Darzynkiewicz Z (1994) Acid-induced denaturation of DNA in situ as a probe of chromatin structure. Methods Cell Biol 41: 527–541

Darzynkiewicz Z, Bruno S, Del Bino G, et al. (1992) Features of apoptotic cells measured by flow cytometry. Cytometry 13: 795–808

Entwistle A, Noble M (1992) The use of polarization analysis in the quantification of fluorescent emission: general principles. J Microsc 165:331–346

Erenpreisa J (1989) Two mechanisms of chromatin compaction. Acta Histochem, 86:129–135

Erenpreisa J (1990) Organization of the chromatin in interphase cell nucleus (in Russian). Zinatne Publishers, Riga

Erenpreisa JA, Zirne RA, Zaleskaya ND, Sjakste TG (1988) Influence of DNA single-strand breaks on ultrastructural organization and cytochemistry of tumour cell chromatin. Bull Exp Biol Med 106:1605–1608

Erenpreisa J, Freivalds T, Selivanova G (1992) Influence of chromatin condensation on the absorption spectra of nuclei stained with toluidine blue. Acta Morphol Hung 40:3–10

Ferlini C, Dicesare S, Rinaldi G, et al. (1996) Flow cytometric analysis of the early phases of apoptosis by cellular and nuclear techniques. Cytometry 24:106–115

Fisher J, Romhanyi G (1977) Optical studies on the molecular-steric mechanism of metachromasia. Acta Histochem 59: 29–39

Förster T, König E (1957) Absorptionspektren und Fluoreszenzeigenschaften in Losungen organischer Farbstoffe. Z Electrochem 61:344–348

Gavrieli Y, Sherman Y, Ben-Sasson SA (1992) Identification of programmed cell death in situ via specific labelling of nuclear DNA fragmentation. J Cell Biol 119:493–501

Ghibelli L, Maresca V, Coppola S, Gualandi G (1995) Protease inhibitors block apoptosis at intermediate stages. A compared analysis of DNA fragmentation and apoptotic nuclear morphology. FEBS Lett 377:9–14

Hotz MA, Gong J, Traganos F, Darzynkiewicz Z (1994) Flow cytometric detection of apoptosis: comparison of the assays of in situ DNA degradation and chromatin changes. Cytometry 15:237–244

Lieger TJ, Hyun W, Yen B, Stittes DS (1995) Detection and quantification of live, apoptotic, and necrotic human peripheral lymphocytes by single-laser flow cytometry. Clin Diagn Lab Immunol 2:369–376

McConkey DJ, Zhivotovsky B, Orrenius S (1996) Apoptosis - molecular mechanisms and biomedical implications. Mol Aspects Med 17:1–110

Michaelis L (1947) The nature of the interaction of nucleic acids and nuclei with basic dyestuffs. Cold Spring Harbor Symp Quant Biol 12:131–142

Pellicciari C, Manfredi AA, Bottone MG, et al. (1993) A single-step staining procedure for the detection and sorting of unfixed apoptotic thymocytes. Eur J Histochem 37:381–390

Rigler R (1966) Microfluorometric characterization of intracellular nucleic acids and nucleoproteins by acridine orange. Acta Physiol Scand Suppl 67:267

Roschlau G (1965) Ein Betrag zum histochemischen Verhalten der Kern DNS in Interphase und Mitoze dargestellt durch kombinierte Saurenhydrolyse und Akridinorangefluoro-chromierung. Histochemistry 5:396–406

Sculthore HH (1978) Metachromasia. Med Lab Sci 35:365–370

Stryer L (1988) Biochemistry, 3rd edn. Freeman, New York

Telford W, King LE, Fraker PJ (1992) Comparative evaluation of several DNA binding dyes in the detection of apoptosis-associated chromatin degradation by flow cytometry. Cytometry 13:137–143

Wyllie AH, Beattie GJ, Hargreaves AD (1981) Chromatin changes in apoptosis. Histochem J 13:681–692